Available online at www.sciencedirect.com
ScienceDirect
Journal of Magnetic Resonance 191 (2008) 7–15
JMR Journal of Magnetic Resonance
www.elsevier.com/locate/jmr

Solid state ^{19}F NMR parameters of fluorine-labeled amino acids. Part I: Aromatic substituents

Ulrich H.N. Dürr [a], Stephan L. Grage [b], Raiker Witter [b], Anne S. Ulrich [b,c,*]

[a] *Max-Planck-Institute for Biophysical Chemistry, Department of NMR-Based Structural Biology, Am Fassberg 11, 37077 Göttingen, Germany*
[b] *Forschungszentrum Karlsruhe, Institute of Biological Interfaces, P.O. Box 3640, 76021 Karlsruhe, Germany*
[c] *University of Karlsruhe, Institute of Organic Chemistry, Fritz-Haber Weg 6, 76131 Karlsruhe, Germany*

Received 14 September 2007; revised 30 October 2007
Available online 3 December 2007

Abstract

Structural parameters of peptides and proteins in biomembranes can be directly measured by solid state NMR of selectively labeled amino acids. The ^{19}F nucleus is a promising label to overcome the low sensitivity of ^{2}H, ^{13}C or ^{15}N, and to serve as a background-free reporter group in biological compounds. To make the advantages of solid state ^{19}F NMR fully available for structural studies of polypeptides, we have systematically measured the chemical shift anisotropies and relaxation properties of the most relevant aromatic and aliphatic ^{19}F-labeled amino acids. In this first part of two consecutive contributions, six different ^{19}F-substituents on representative aromatic side chains were characterized as polycrystalline powders by static and MAS experiments. The data are also compared with results on the same amino acids incorporated in synthetic peptides. The spectra show a wide variety of lineshapes, from which the principal values of the CSA tensors were extracted. In addition, temperature-dependent T_1 and T_2 relaxation times were determined by ^{19}F NMR in the solid state, and isotropic chemical shifts and scalar couplings were obtained in solution.

Keywords: Fluorine; Solid state NMR; Amino acid; ^{19}F chemical shift anisotropy

1. Introduction

A serious limitation in solid state NMR studies of biological systems is the intrinsically low sensitivity of this spectroscopic technique. In particular, the low gyromagnetic ratio of most conventionally used isotope labels (^{15}N, ^{13}C, and ^{2}H) results in a poor signal-to-noise ratio, and their dipolar interactions cover only a relatively short distance range. To improve this situation, ^{19}F is increasingly being employed as an alternative reporter nucleus in NMR studies of biopolymers (for reviews, see e.g. [1–5]). Using this label, sensitivity enhancements of 1–2 orders of magnitude are readily achieved [6], and distance ranges of up to ~14 Å (as opposed to ~7 Å with conventional labels) are possible [7–9]. Recent studies have demonstrated the feasibility of ^{19}F NMR for biomembrane studies, suggesting that any structural perturbations by ^{19}F-substituents are not usually significant for aliphatic and aromatic amino acids of similar size [6,10–18].

A wide variety of ^{19}F-labeled amino acids can be incorporated into polypeptides by solid-phase peptide synthesis, and some of them are even suitable for biosynthetic labeling in *Escherichia coli* (e.g. fluoro-tryptophan, fluoro-phenylalanine, fluoro-tyrosine, fluoro-leucine, fluoro-histidine) [19–38]. Selective ^{19}F-labels in side chains are readily used as highly sensitive probes to characterize the local conformation and dynamics [39]. In those cases where the ^{19}F-label is attached to the polypeptide backbone in a well-defined and rigid geometry, it is even possible to describe the orientation and mobility of a given secondary structure element in a lipid membrane [6,10–12,17,18,40–42]. In order to make use of the advantages of ^{19}F NMR, however, detailed knowledge of the NMR parameters of the labels is necessary, which are in many cases not readily

* Corresponding author. Address: Forschungszentrum Karlsruhe, Institute of Biological Interfaces, P.O. Box 3640, 76021 Karlsruhe, Germany.
E-mail address: anne.ulrich@ibg.fzk.de (A.S. Ulrich).

1090-7807/$ - see front matter © 2007 Elsevier Inc. All rights reserved.
doi:10.1016/j.jmr.2007.11.017

available. As a basis for further solid state ^{19}F NMR studies in biological systems we have therefore recorded and compiled the chemical shift anisotropies, the isotropic chemical shifts, and the relaxation properties of the most prominent polycrystalline ^{19}F-labeled amino acids. Aromatic amino acids with a ^{19}F-substituent on the ring are discussed in the present contribution (Part I). This set of data includes most of the amino acids that are suitable for biosynthetic labeling. Part II then characterizes amino acids containing aliphatic ^{19}F-labels, with an emphasis on CF_3-groups [43].

The fluorine-labeled amino acids studied here, with single ^{19}F-substituents on phenyl- and indole-rings, are illustrated in Fig. 1. Two derivatives of phenylalanine (3F-Phe and 4F-Phe, with a fluorine label in the *meta*- and *para*-position, respectively), and a tyrosine analogue (4F-Tyr) were characterized. Another, more unusual phenyl-substituted amino acid, 4-fluoro-phenylglycine (4F-Phg), is of particular interest for distance measurements, since the position of the ^{19}F-label is fixed and geometrically well-defined with respect to the peptide backbone. Furthermore, two tryptophan analogues (5F-Trp and 6F-Trp) are included, which have found widespread use in biological applications of ^{19}F NMR [20,22,23,25,28,29,31,36,39].

2. Materials and methods

2.1. Amino acids

The amino acids and their abbreviations are summarized in Fig. 1 (for stereoisomers see Table 1). 4F-Phe and 4F-Phg were purchased from Fluka, 3F-Tyr and 5F-Trp (racemic mixture) from Lancaster, and 6F-Trp (racemic mixture) from Acros. 5F-L-Trp and 6F-L-Trp was provided by T. A. Cross (Tallahassee, USA) and 3F-Phe was a gift from T. Asakura (Tokyo, Japan). All polycrystalline ^{19}F-labeled amino acids were used as obtained from the suppliers.

2.2. NMR measurements

Most ^{19}F NMR solid state NMR spectra were recorded at 20 °C on a wide bore Bruker Avance spectrometer (Bruker BioSpin GmbH, Rheinstetten, Germany) operating at a ^{19}F resonance frequency of 564.7 MHz. A double tuned (^{19}F/^{1}H) Bruker 4 mm MAS probe was used with ^{19}F 90° pulses of 2 μs and ^{1}H-decoupling of 40 kHz. Static spectra were acquired using a Hahn echo sequence with an echo delay of 25 μs. Magic angle spinning NMR spectra were obtained at 12.5 kHz spinning speed, using a single pulse excitation following saturation by a 90° pulse train. The ^{19}F NMR relaxation measurements and spectra shown in Fig. 3 were performed at 470.3 MHz ^{19}F resonance frequency on a Varian Unity Inova spectrometer (Varian Inc., Palo Alto, CA) equipped with an Oxford Instruments wide bore magnet. Here, a double-tuned (^{1}H/^{19}F) static flat-coil probe from Doty Scientific (Columbia, SC, USA) was used with proton-decoupling up to 40 kHz and ^{19}F 90° pulse lengths between 2 and 3 μs. (Note, that due to the proximity of the ^{19}F and ^{1}H resonance frequencies the hardware requirements for high power ^{1}H-decoupling are demanding, and the relatively moderate decoupling levels achieved here are hence not reaching the values often employed in e.g. ^{13}C NMR) The T_1 values were mostly determined by inversion recovery (only in the case of very long T_1 by saturation recovery), and the T_2 data was acquired using a Hahn echo experiment. Relaxation times were measured in the temperature range from −60 to +60 °C with an accuracy of ±2 °C. Liquid state ^{19}F NMR spectra were collected at 470 MHz on a Varian Ino-

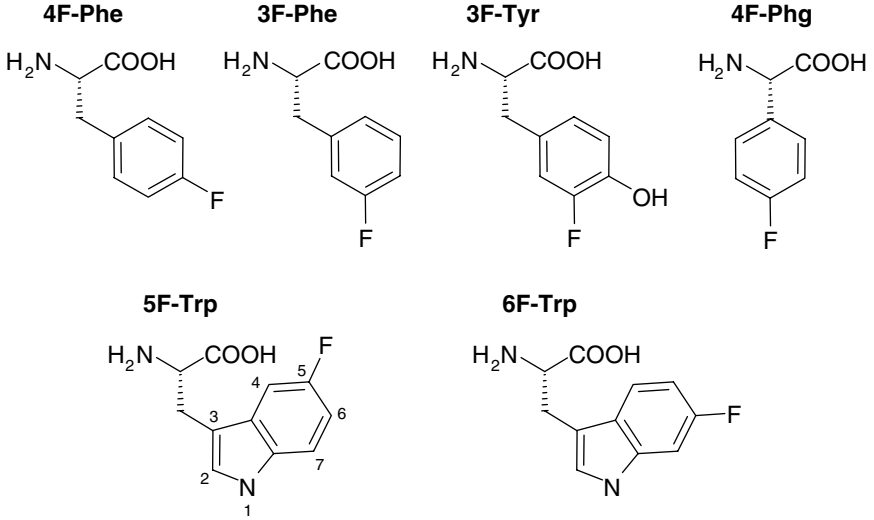

Fig. 1. Structures of the ^{19}F-labeled amino acids carrying a single fluorine substituent on an aromatic ring: 4-fluoro-phenylalanine (4F-Phe), 3-fluoro-phenylalanine (3F-Phe), 3-fluoro-tyrosine (3F-Tyr), 4-fluoro-phenylglycine (4F-Phg), 5-fluoro-tryptophan (5F-Trp), and 6-fluoro-tryptophan (6F-Trp). Shown are the L-stereoisomers.

va widebore spectrometer using a 5 mm liquid state probe, or at 376 MHz on a Bruker standard bore DMX spectrometer. All ^{19}F NMR spectra are referenced with $CFCl_3$ set to 0 ppm (using in the solid state NMR experiments as secondary standard 100 mM NaF at 25 °C, set to −119.5 ppm).

2.3. Data analysis

The principal values of the ^{19}F chemical shift tensors were obtained from the intensities of the spinning sidebands using the Herzfeld–Berger algorithm [44], as implemented in the program "HBA", version 1.2 (Klaus Eichele, R.E. Wasylishen, Dalhousie University and Universität Tübingen). Two or three spinning sidebands on either side of the center band were used, which Hodgkinson and Emsley [45] have found to be optimal for a reliable determination of the CSA tensor principal values. The spinning sideband intensities and positions were determined by fitting the experimental NMR spectra with simulated lines using Lorentzian or Gaussian functions. The tabulated chemical shift values were derived from the fits with Gaussian lines. Alternative fits using Lorentzian lines gave deviations below 0.5 ppm whenever three or more sidebands could be fitted on each side of the isotropic line. The error inherent in the spectral signal-to-noise and other imperfections will add to this, hence we estimate the overall error of the reported chemical shift values to be of the order of ±2 ppm. For the lineshape simulations we employed the Origin data processing package version 7 (OriginLab Coop., Northampton, MA), extended by the ONMR module (www.nmrtools.com). Some spectra consisted of several sideband families originating from different polymorphic contributions, which were fitted by a superposition of an appropriate number of sideband patterns.

The chemical shift tensors were characterized by their three principal values δ_{11}, δ_{22}, δ_{33}, using the convention $\delta_{11} > \delta_{22} > \delta_{33}$, by their isotropic chemical shift $\delta_{iso} = (\delta_{11} + \delta_{22} + \delta_{33})/3$, by their anisotropy defined as $\Delta = \delta_{11} - \delta_{iso}$ if $|\delta_{11} - \delta_{iso}| > |\delta_{33} - \delta_{iso}|$ and $\Delta = \delta_{33} - \delta_{iso}$ otherwise, as well as their asymmetry $\eta = |\delta_{22} - \delta_{33}|/|\delta_{11} - \delta_{iso}|$ if $|\delta_{11} - \delta_{iso}| > |\delta_{33} - \delta_{iso}|$ and $\eta = |\delta_{22} - \delta_{11}|/|\delta_{33} - \delta_{iso}|$ otherwise.

3. Results and discussion

3.1. Liquid state NMR

A list of all amino acids that have been characterized here is compiled in Table 1, together with their ^{19}F NMR parameters obtained in aqueous solution. The isotropic chemical shift values (δ_{iso}), J-coupling constants, and the types of multiplet were determined. Even though ^{19}F is known for its large chemical shift dispersion, the shifts of the aromatic amino acids studied here cover a moderate range from −112 to −125 ppm (relative to $CFCl_3$), in agreement with literature values on related aromatic compounds [46,47]. The chemical shifts of a single fluorine substituent on the phenyl rings of 3F-Phe, 4F-Phe or 4F-Phg were found to be around −112 to −116 ppm and did not show a strong variation. Whether fluorine is substituted in the *meta*- or *para*-position has only a minor influence on the observed chemical shift. In the case of tyrosine, where the phenyl ring carries an additional hydroxyl group, the resonance is shifted to −137 ppm. Fluorine substituents on the indole side chain of tryptophan resonated between −121 and −124 ppm.

3.2. ^{19}F CSA tensors of polycrystalline powders

Solid state ^{19}F NMR spectra of the fluorinated amino acids as polycrystalline powders were recorded in a static mode as well as by magic angle spinning at 12.5 kHz (see Figs. 2 and 3 for representative spectra). Repeatedly, the static ^{19}F NMR spectra did not exhibit any typical powder patterns that would have been expected for a single chemical shift tensor. Instead, the distorted lineshapes contained several tensor contributions originating from different crystal forms present in the same powder sample. Without having to re-crystallize the polymorphic samples into a uniform crystal modification, it was possible to separate the different spectral components using MAS ^{19}F NMR. To achieve the necessary resolution whilst maintaining enough spinning sidebands for extracting the chemical shift

Table 1
^{19}F NMR parameters of aromatic amino acids with ^{19}F-substituents, measured in aqueous solution (~0.01 mg/ml, room temperature)

Substance	Chirality	δ_{iso} (ppm)	^{1}J (Hz)	^{2}J (Hz)	Type of spectrum
4F-Phe	L	−115.76	8.5	4.5	Triplet of triplets
	D/L	−115.67			Not resolved[a]
3F-Phe	Unknown	−113.33	9.8	6.8	Triplet of doublets
3F-Tyr	D/L	−136.70	8.8	3.6	Doublet of doublets
4F-Phg	D/L	−112.55	8.8	4.5	Triplet of triplets
5F-Trp	L	−124.91	9.6	4.6	Triplet of doublets
	D/L	−124.82			Not resolved[a]
6F-Trp	L	−122.18			Not resolved[a]
	D/L	−121.70	9.4	5.3	Triplet of doublets

[a] Data acquired on a 400 MHz spectrometer did not provide the necessary resolution, all other data was obtained on a 500 MHz spectrometer.

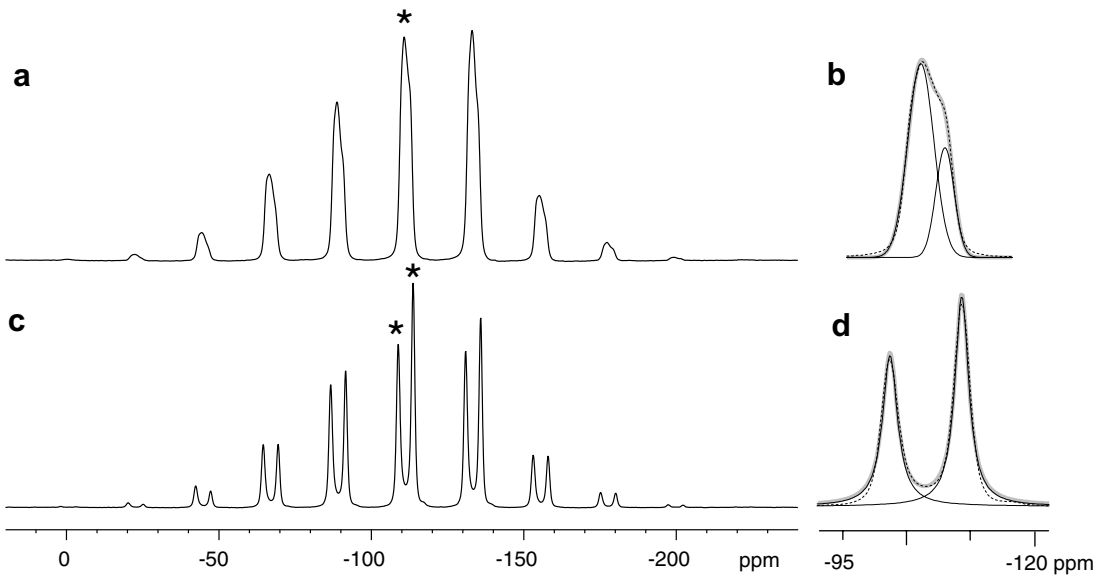

Fig. 2. Chemical shift parameters were obtained from ^{19}F NMR MAS spectra (12.5 kHz, 564.7 MHz resonance frequency). This way, multiple spectral components arising from different crystal forms in the polymorphic samples could be distinguished, as illustrated here for 4F-Phe in the pure L-form (a and b) and the racemic D/L-mixture (c and d). The relative intensities were determined by best-fit analysis of the lines, as shown for the centerband (indicated by *) of the L-enantiomer (b) and the racemic mixture (d), using Gaussian (b) or Lorentzian (d) functions (dashed: experimental data; solid: individual fitted lines; grey: sum of fitted lines).

tensor values, the use of a high-field magnet (14.1 T) was essential. As an example, Fig. 2 shows the MAS spectra of 4F-Phe both as a pure L-enantiomer and a racemic D/L-mixture (a and c, respectively), in which multiple sets of MAS sideband patterns are sufficiently resolved (b and d). The sideband intensities could thus be analyzed to determine the CSA tensor principal components using the Herzfeld–Berger algorithm [44]. The principal values δ_{11}, δ_{22}, δ_{33} determined this way for every polymorphic constituent, as well as the isotropic chemical shift δ_{iso}, the anisotropy Δ, and the asymmetry η as defined in Section 2, are compiled in Table 2.

The isotropic chemical shift values determined in the solid state and in aqueous solution tend to be very similar within a couple of ppm most of the time, but in a few cases were found to differ by up to 10 ppm. For other isotopes a closer agreement between NMR in the solid state and in solution is usually observed, but the ^{19}F nucleus is known to be particularly sensitive towards its local environment [47]. The three lone pairs of electrons on the aromatic ^{19}F-substituent are strongly affected by the local packing in a crystalline environment, by the polarity and type of solvent, by hydrogen-bonding effects, and by temperature.

The isotropic chemical shift values of the ^{19}F-substituents on phenyl side chains are found to be centred around $\delta_{iso} = -110$ ppm, with the exception of tyrosine, where the additional OH-group moves the value to $\delta_{iso} = -135$ ppm, in good agreement with the data in aqueous solution. Large spectral widths were observed for these amino acids, characterized by an anisotropy Δ ranging from 55 to 75 ppm. Their CSA tensors are highly asymmetric with η between 0.48 and 0.97. The range of chemical shift parameters within any polymorphic crystal modifications of 4F-Phe, 3F-Phe or 4F-Phg was found to be of a similar extent as the differences between these amino acids themselves, indicating a significant influence of the crystal environment on the chemical shift. As found for the isotropic chemical shifts, also the anisotropy and asymmetry of 4F-Tyr are influenced by the OH-group, and the anisotropy of $\Delta = -75$ ppm, as well as the significantly lower asymmetry of $\eta = 0.48$ are clearly different from the other phenyl-derivatives.

In 5F- and 6F-Trp, isotropic chemical shift values around $\delta_{iso} = -120$ ppm were observed, each being about 2 ppm higher than the value in aqueous solution. All anisotropies Δ amount to around 50 ppm. For the value of η, however, a remarkable difference between the analogues substituted in 5- and 6-position is found. The 5F-Trp analogues display a very small asymmetry $\eta \approx 0$ (for the crystal form used for the MAS experiments, see below), while both analogues labeled in the 6-position are characterized by a high asymmetry around $\eta \approx 0.7$. In both cases of 6F-Trp the MAS spectra consist of two components, which overlapped and could not be resolved by line-fitting. Therefore the error associated with these principal tensor values is considerably larger than for the other amino acids. Still, the static spectra of 6F-Trp (data not shown) clearly confirmed the large asymmetry of the CSA tensors.

3.3. Influence of the external environment on the ^{19}F chemical shift

The considerable dependency of fluorine chemical shifts on the local molecular environment raises the question as

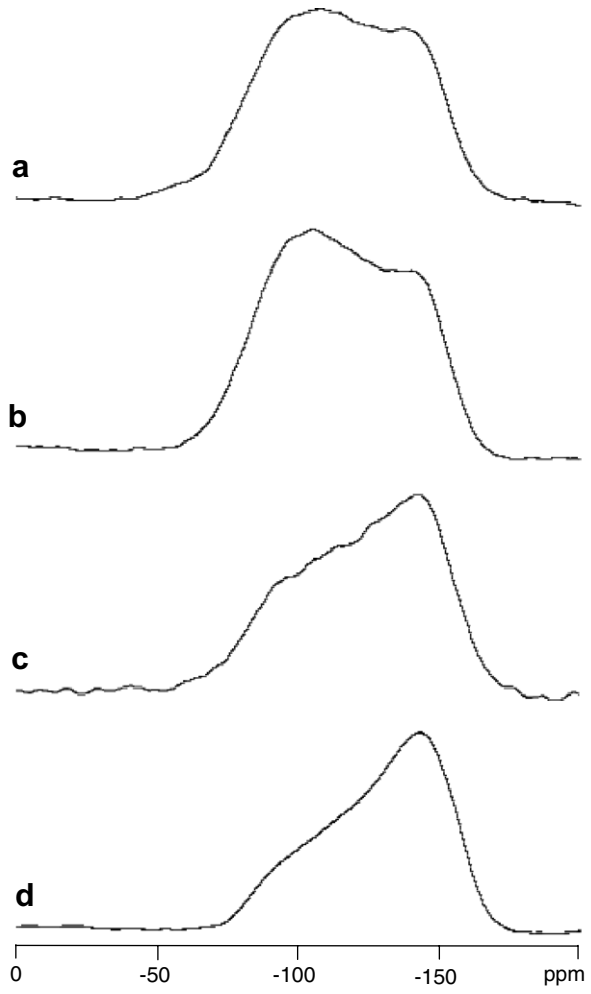

Fig. 3. ^{19}F NMR spectra of polycrystalline racemic 5F-Trp re-crystallized from different solvents, namely ethanol (a), methanol (b), and water (c). The spectrum (d) of lyophilized gramicidin A labeled with 5F-Trp in position 13 exemplifies the well-defined lineshapes that were generally observed for lyophilized peptides.

to what extent the parameters obtained from pure amino acids can be applied to peptides and proteins. In order to analyze biological ^{19}F NMR samples on the basis of the chemical shifts obtained here from the pure amino acids, the differences within any polycrystalline amino acid and with respect to the corresponding polypeptide side chain should be sufficiently small. To address these two issues, we examined the ^{19}F chemical shifts of various tryptophan preparations in more detail, and we compared the parameters of pure amino acids with those of several ^{19}F-labeled peptides.

As noted above, a polycrystalline sample often exhibited several different CSA tensors, and the variations within one sample sometimes even exceeded the differences between different amino acids. As a first attempt to reduce the influence of crystal packing on the chemical shift and to imitate a more homogeneous environment, some of the ^{19}F-labeled amino acids were lyophilized. This procedure did not improve the spectra but instead yielded featureless lineshapes, reflecting an even more diverse molecular environment in a lyophilisate (but see below that lyophilized *peptide* samples yielded well-defined CSA tensors). A better approach to generate homogeneous samples was to re-crystallize the amino acids from different solvents. Fig. 3 shows that the ^{19}F NMR spectra of 5F-D/L-Trp re-crystallized from ethanol, methanol, and water differ considerably. In particular the samples from ethanol and methanol (Fig. 3a and b) display a pronounced hump on the low-field side, suggesting a component with $\eta \approx 1$ in addition to the previously characterized tensor pattern with $\eta \approx 0$ seen by MAS. Only the lineshape of the material re-crystallized from H_2O (Fig. 3c) shows a single contribution with the same low asymmetry as found by MAS, and it also closely resembles the spectrum of 5F-Trp incorporated in the lyophilized peptide gramicidin A [39] (Fig. 3d). The corresponding chemical shift tensor values also compare fairly well with other studies on polycrystalline 5F-Trp ($\delta_{11} = -73.9$ ppm, $\delta_{22} = -150.1$ ppm, $\delta_{33} = -155.4$ ppm, Δ=52.6 ppm, $\eta = 0.10$) [48] and single crystals of 5F-Trp ($\delta_{11} = -75.6$ ppm, $\delta_{22} = -139.8$ ppm, $\delta_{33} = -159.4$ ppm, $\Delta = 49.3$ ppm, $\eta = 0.40$) [49], except for the lower asymmetry encountered in our study. It thus appears that different crystal forms within the same polycrystalline powder are responsible for the multi-component lineshapes, which would be consistent with a previous report that phenylalanine forms different morphologies when re-crystallized from H_2O or methanol/H_2O mixtures [50]. Another possible explanation for the pronounced deviations from a simple powder pattern (Fig. 3a and b) could be differential motional averaging of the 5F-Trp molecules in their crystal sites, which, however, would be in disagreement with recent observations on crystalline 5F-Trp by other groups [49,51]. Dipolar couplings between ^{19}F nuclei that are in close spatial proximity in the lattice could also be responsible for the observed unusual lineshapes. However, they seem unlikely since we found that co-crystallization of 5F-D/L-Trp with unlabeled Trp at a molar ratio of 1:10 did not change the distorted lineshapes.

Next, consider the non-natural amino acid 4F-L-Phg, which has also been incorporated as a ^{19}F NMR label into several different polypeptides [10,12,40]. In all these peptide samples, the static spectra had exhibited well-defined tensor lineshapes from which the principal CSA chemical shift values could be readily extracted by fitting (data not shown). This behaviour is in stark contrast to the results from the polycrystalline state described here. Nonetheless it is now possible to compare the ^{19}F NMR parameters determined for polycrystalline 4F-Phg (Table 2) with the data of a single 4F-Phg label incorporated in the fusogenic peptide B18 at eight different positions, and in the antimicrobial peptide Gramicidin S at two different sites (Table 3) [10,12,40]. To eliminate motional averaging effects we acquired the spectra on immobilized peptides, namely lyophilized B18 and gramicidin S embedded in DMPC membranes in the gel-state. The chemical shift values in these 10 different polypeptides are found to be quite similar within 3 ppm (see Table 3). On the other hand, for the

Table 2
Solid state ^{19}F NMR parameters of polycrystalline amino acids, extracted from MAS spectra at 20 °C by Herzfeld–Berger analysis

Substance	Chirality	δ_{11} (ppm)	δ_{22} (ppm)	δ_{33} (ppm)	δ_{iso} (ppm)	Δ (ppm)	η	T_1 (s)	T_2 (μs)
4F-Phe	L	−51.9	−118.4	−162.0	−110.8	58.9	0.74	352 ± 12[a]	33.8 ± 0.8
		−41.6	−124.5	−171.4	−112.5	70.9	0.66		
	D/L	−48.4	−114.2	−164.0	−108.9	60.5	0.82	75.5 ± 3.0	40.6 ± 7.2
		−56.7	−120.9	−163.8	−113.8	57.1	0.75		
3F-Phe	Unknown	−54.7	−115.2	−156.5	−108.8	54.1	0.76	91 ± 11	39.4 ± 3.8
		−55.7	−121.3	−158.4	−111.8	56.1	0.66		
		−57.6	−123.4	−159.6	−113.5	55.9	0.65		
3F-Tyr	D/L	−79.9	−115.7	−209.7	−135.1	−74.6	0.48	14.9 ± 0.7[a]	25.4 ± 5.4
4F-Phg	L	−46.6	−109.3	−168.8	−108.2	61.6	0.97	7.68 ± 0.3	37.8 ± 3.2
		−51.6	−117.5	−162.7	−110.6	59.0	0.77		
		−55.4	−125.8	−161.7	−114.3	58.9	0.61		
	D/L	−53.1	−118.7	−165.0	−112.2	59.2	0.78	36.6 ± 4.7	23.6 ± 1.2
5F-Trp	L	−70.9	−146.8	−148.7	−122.1	51.2	0.04	133.6 ± 4.5	37.6 ± 0.8
	D/L	−77.5	−148.2	−148.2	−124.6	47.1	0.00	27.5 ± 1.2	42.0 ± 1.1
6F-Trp	L	−66.9	−127.5	−162.6	−119.0	52.1	0.67	52.3 ± 5.4	31.4 ± 5.2
	D/L	−67.7	−125.7	−163.9	−119.1	51.4	0.74	104.8 ± 6.3	26.7 ± 1.7

[a] Obtained at 0 °C.

Table 3
CSA values of 4F-Phg and 5F-Trp incorporated in various polypeptides, lyophilized or reconstituted in DMPC membranes in the gel-state (5 °C)

Peptide	Label	Position	Condition	δ_{11} (ppm)	δ_{22} (ppm)	δ_{33} (ppm)	δ_{iso} (ppm)	Δ (ppm)	η
B18 [12]	4F-Phg	Average[a]	Lyophilized	−60.1	−124.3	−155.3	−113.2	53.1	0.58
Gramicidin S[10,40]	4F-Phg	Leu3/3′	membrane-bound	−65.5	−126.5	−153.0	−115.0	49.5	0.54
Gramicidin A[39,52]	5F-Trp	Trp13	Lyophilized	−85	−143	−160	−129	44.0	0.38
Gramicidin A[39,52]	5F-Trp	Trp13	Membrane-bound	−80.0	−141.5	−156.5	−126.0	46.0	0.33
Gramicidin A[39,52]	5F-Trp	Trp15	Membrane-bound	−81.0	−141.0	−157.5	−126.5	45.5	0.36
GB1[53,54]	5F-Trp	Trp43	Aqueous solution	–	–	–	−124.2	–	–
GB1[54]	5F-Trp	Trp43	Lyophilized	−82.7	−140.2	−151.8	−124.9	42.2	0.27

[a] The ^{19}F NMR chemical shift parameters of B18 labeled in positions 103, 105, 106, 107, 110, 116, 117, 118 have been averaged, as the respective values are all within 3 ppm from each other.

polycrystalline amino acid the isotropic chemical shift δ_{iso} occurs over range of 7 ppm centred around 111 ppm, depending on the local crystalline environment, and the principal CSA values vary up to 16 ppm (see Table 2). This observation suggests that the environment of a lyophilized or membrane-embedded peptide is more homogeneous compared to a densely packed aromatic crystal. Table 3 also shows that the anisotropy Δ is reduced by about 15% in the peptides compared to the polycrystalline amino acid, due to some residual mobility in the peptide samples.

Since tryptophan plays an important role in anchoring membrane proteins at the polar/apolar interface of the lipid bilayer, its side chain conformation has been characterized in detail, e.g. in the peptide gramicidin A [39,52]. Fluorine-labeled tryptophan can also be conveniently incorporated biosynthetically into proteins for ^{19}F NMR, as demonstrated e.g. with the soluble protein GB1 [53,54]. Table 3 compares the chemical shift parameters of 5F-Trp in such biological samples, either in the lyophilized form or embedded in gel-state DMPC membranes (a representative powder spectrum was shown in Fig. 3d) The chemical shift values in the different polypeptide preparations show a similar variability as in the polycrystalline amino acid, with δ_{iso} occurring near −125 ppm over a 7 ppm range. As noted above, the molecular motions in a polypeptide are not completely suppressed by lyophilization or in a gel-state membrane, giving rise to somewhat reduced anisotropies Δ. The asymmetry parameter of 5F-Trp in peptides (η between 0.3 and 0.6) is found to be significantly higher than in the nearly symmetric polycrystalline 5F-Trp (though still lower than in 6F-Trp with $\eta \approx 0.7$). Again, the chemical shift tensors of the various peptides show less variation than the polycrystalline amino acid itself, which was found to be highly susceptible to the differences in molecular environment when crystallized from different solvents (Fig. 3). A polypeptide thus seems to provide a more homogeneous environment than an aromatic polycrystalline sample. Likewise, a recent study [49] on single crystals of 5F-Trp yielded chemical shift tensor values similar to those obtained here for 5F-Trp in gramicidin A, lending support to this interpretation because a single crystal environment is also more homogeneous than a polycrystalline sample.

3.4. Relaxation

The longitudinal relaxation times T_1 of the aromatic ^{19}F-labeled amino acids were recorded as a function of temperature in the range of −60 to +60 °C, as illustrated in Fig. 4. The values of T_1 and T_2 at 20 °C are explicitly stated in Table 2. For T_2 relaxation no significant temperature dependence was found, and the values do not differ much amongst the various amino acids (20–40 μs), as they are dominated by the proximity of neighboring protons in these polycrystalline organic compounds. In contrast, the T_1 relaxation times exhibit a pronounced temperature dependency. Except for 3F-Tyr, remarkably long T_1 relaxation times were observed for the aromatic ^{19}F amino acids investigated here, especially at low temperature. Such long T_1 values of several 100 s suggest a virtually complete lack of motion of the packed aromatic rings. Almost all T_1-values of the aromatic ^{19}F-substituents decrease with increasing temperature within the accessible range, placing any putative T_1-minimum at temperatures above 60 °C. The motions leading to T_1 relaxation in the observed temperature range are thus slower than the Larmor frequency of 470.3 MHz.

4. Conclusions

To compile a database of ^{19}F NMR parameters of the most prominent ^{19}F-labeled amino acids we have measured here the chemical shift parameters of aromatic amino acids carrying a single ^{19}F-substituent on a phenyl or indole ring. In several cases the polycrystalline powders displayed a pronounced polymorphism, which lead to a considerable spread in the chemical shift parameters within any one kind of amino acid. Nonetheless, the local molecular environment provided by different ring systems is reflected in characteristic and distinct chemical shift parameters. For example, the isotropic chemical shifts can be grouped according to the influence of neighboring substituents on the ^{19}F-label, namely as 4F-Phe, 3F-Phe and 4F-Phg (with shifts between −108 and −114 ppm), 6F- and 5F-Trp (−119 to −125 ppm), and 4F-Tyr (−135 ppm). The anisotropies cover a range of 45–75 ppm, and the values of any one polymorphic amino acid vary less than ∼5 ppm, with the exception of the 4F-Phe crystal forms for which they exhibit a larger spread. Strong variations were generally encountered for the asymmetry parameter, which was large (0.5–1.0) for most samples, except for certain crystal forms of 5F-Trp with a nearly symmetric CSA tensor. Remarkable in this context is the difference between the two tryptophan analogues, adopting two extreme asymmetry parameters of ∼0 (5F-Trp) and 1.0 (6F-Trp). Altogether, the isotropic chemical shift is the most characteristic and well conserved parameter in the solid state, and a good agreement is demonstrated here also with the values observed in aqueous solution.

To judge whether the chemical shift parameters obtained from the crystalline amino acids can be applied to ^{19}F-labeled proteins, the ^{19}F NMR data of several peptides labeled with 4F-Phg or 5F-Trp were included in this compilation. The chemical shift values amongst these preparations were more homogeneous than within the polycrystalline amino acids, suggesting that it is better to use the tabulated values (or newly acquired parameters) of the lyophilized peptide samples than of the polycrystalline amino acids, in contrast to the aliphatic amino acids discussed in Part II [43]. Nonetheless, the chemical shift anisotropies Δ of the pure aromatic amino acids give some clues for biological samples, taking into account differences due to residual molecular motion in the peptide samples. In the case of T_1 and T_2 relaxation times, a transfer of the data from polycrystalline amino acids to the side chains of polypeptides is not reasonable because of the very different motional properties. Fortunately, the extremely long T_1-times observed here in polycrystalline amino acids have never been encountered in any of our biomolecular samples to date (typical relaxation times ∼1 s), thus ^{19}F NMR remains a method of choice for rapid acquisition of highly sensitive and background-free spectra.

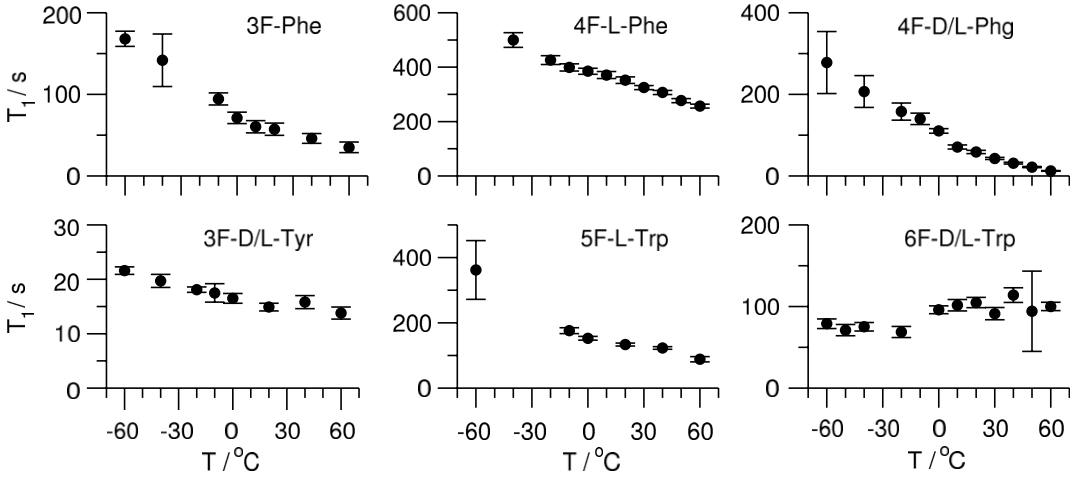

Fig. 4. Temperature dependence of the T_1 relaxation times of the aromatic ^{19}F-substituents.

Acknowledgments

We thank Prof. T. Asakura (Tokyo University of Agriculture and Technology) for the gift of 3F-Phe, and Prof. T. Cross (Florida State University, NHFML) for 5F-L-Trp and 6F-L-Trp. The authors gratefully acknowledge the Deutsche Forschungsgemeinschaft for financial support of SFB 197 (TP B13) and the Center for Functional Nanostructures (E1.2).

References

[1] J.T. Gerig, Fluorine NMR of proteins, Prog. NMR Spectrosc. 26 (1994) 293–370.
[2] A.S. Ulrich, Solid state ^{19}F NMR methods for studying biomembranes, Prog. Nucl. Magn. Reson. Spectr. 46 (2005) 1–21.
[3] A.S. Ulrich, P. Wadhwani, U.H.N. Dürr, S. Afonin, R.W. Glaser, E. Strandberg, P. Tremouilhac, C. Sachse, M. Berditchevskaia, S. Grage, Solid state ^{19}F NMR analysis of membrane-active peptides, in: A. Ramamoorthy (Ed.), NMR Spectroscopy of Biological Solids, Taylor & Francis, London, 2006, pp. 215–236.
[4] A.S. Ulrich, Solid state ^{19}F NMR analysis of oriented biomembranes, in: G.A. Webb (Ed.), Modern Magnetic Resonance, Springer, 2007, pp. 257.
[5] A.S. Ulrich, High resolution ^{1}H and ^{19}F solid state NMR, in: J. Lindon, G. Tranter, J. Holmes (Eds.), Encyclopedia of Spectroscopy and Spectrometry, Academic Press, London, 2000, pp. 813–825.
[6] S.L. Grage, A.V. Suleymanova, S. Afonin, P. Wadwhani, A.S. Ulrich, Solid state NMR analysis of the dipolar couplings within and between distant CF_3-groups in a membrane-bound peptide, J. Magn. Reson. 183 (2006) 77–86.
[7] M.L. Gilchrist, K. Monde, Y. Tomita, T. Iwashita, K. Nakanishi, A.E. McDermott, Measurement of interfluorine distances in solids, J. Magn. Reson. 152 (2001) 1–6.
[8] E.A. Louie, P. Chirakul, V. Raghunathan, S.T. Sigurdsson, G.P. Drobny, Using solid-state ^{31}P{^{19}F} REDOR NMR to measure distances between a trifluoromethyl group and a phosphodiester in nucleic acids, J. Magn. Reson. 178 (2006) 11–24.
[9] G.L. Olsen, E.A. Louie, G.P. Drobny, S.T. Sigurdsson, Determination of DNA minor groove width in distamycin-DNA complexes by solid-state NMR, Nucleic Acids Res. 31 (2003) 5084–5089.
[10] S. Afonin, U.H.N. Dürr, P.Wadhwani, J.B. Salgado, A.S. Ulrich, Solid state NMR structure analysis of the antimicrobial peptide Gramicidin S in lipid membranes: concentration-dependent re-alignment and self-assembly as a ß-barrel, in: T. Peters (Ed.), Bioactive Conformation II, Topics in Current Chemistry, vol. 273, in press.
[11] E. Strandberg, P. Wadhwani, P. Tremouilhac, U.H.N. Dürr, A.S. Ulrich, Solid state NMR analysis of the PGLa peptide orientation in DMPC bilayers: structural fidelity of ^{2}H-versus high sensitivity of ^{19}F NMR, Biophys. J. 90 (2006) 1676–1686.
[12] S. Afonin, U.H.N. Dürr, R.W. Glaser, A.S. Ulrich, 'Boomerang'-like insertion of a fusogenic peptide in a lipid membrane revealed by solid-state ^{19}F NMR, Magn. Reson. Chem. 42 (2004) 195–203.
[13] P. Wadhwani, S. Afonin, M. Ieronimo, J. Bürck, A.S. Ulrich, Optimized protocol for synthesis of cyclic gramicidin S: starting amino acid is key to high yield, J. Org. Chem. 71 (2006) 55–61.
[14] O. Toke, R.D. O'Connor, T.K. Weldeghiorghis, W.L. Maloy, R.W. Glaser, A.S. Ulrich, J. Schaefer, Structure of (KIAGKIA)(3) aggregates in phospholipid bilayers by solid-state NMR, Biophys. J. 87 (2004) 1397.
[15] R.W. Glaser, M. Grüne, C. Wandelt, A.S. Ulrich, Structure analysis of a fusogenic peptide sequence from the sea urchin fertilization protein binding, Biochemistry 38 (1999) 2560–2569.
[16] R.W. Glaser, C. Sachse, U.H.N. Dürr, P. Wadhwani, A.S. Ulrich, Orientation of the antimicrobial peptide PGLa in lipid membranes determined from ^{19}F NMR dipolar couplings of 4-CF_3-phenylglycine labels, J. Magn. Reson. 168 (2004) 153–163.
[17] R.W. Glaser, C. Sachse, U.H.N. Dürr, P. Wadhwani, S. Afonin, E. Strandberg, A.S. Ulrich, Concentration-dependent realignment of the antimicrobial peptide PGLa in lipid membranes observed by solid-state ^{19}F NMR, Biophys. J. 88 (2005) 3392–3397.
[18] R.W. Glaser, C. Sachse, U.H.N. Dürr, P. Wadhwani, A.S. Ulrich, Orientation of the antimicrobial peptide PGLa in lipid membranes determined from ^{19}F NMR dipolar couplings of 4-CF_3-phenylglycine labels, J. Magn. Reson. 168 (2004) 153–163.
[19] F. Khan, I. Kuprov, T.D. Craggs, P.J. Hore, S.E. Jackson, ^{19}F NMR studies of the native and denatured states of green fluorescent protein, J. Am. Chem. Soc. 128 (2006) 10729–10737.
[20] G.R. Winkler, S.B. Harkins, J.C. Lee, H.B. Gray, Alpha-synuclein structures probed by 5-fluorotryptophan fluorescence and ^{19}F NMR spectroscopy, J. Phys. Chem. B 110 (2006) 7058–7061.
[21] J.F. Eichler, J.C. Cramer, K.L. Kirk, J.G. Bann, Biosynthetic incorporation of fluorohistidine into proteins in *E. coli*: a new probe of macromolecular structure, ChemBioChem 6 (2005) 2170–2173.
[22] G.L. Abbott, G.E. Blouse, M.J. Perron, J.D. Shore, L.A. Luck, A.G. Szabo, ^{19}F NMR studies of plasminogen activator inhibitor-1, Biochemistry 43 (2004) 1507–1519.
[23] Q. Li, H.Y. Hu, W.Y. Sheng, X.Y. Zhao, G.J. Xu, Study of the structural environment of DsbA protein by labeling of tryptophan analogs, Prog. Biochem. Biophys. 29 (2002) 319–322.
[24] C.M. Dupureur, L.M. Hallman, Effects of divalent metal ions on the activity and conformation of native and 3-fluorotyrosine-PvuII endonucleases, Eur. J. Biochem. 261 (1999) 261–268.
[25] C.Y. Wong, M.R. Eftink, Incorporation of tryptophan analogues into staphylococcal nuclease, its V66W mutant, and Delta 137–149 fragment: spectroscopic studies, Biochemistry 37 (1998) 8938–8946.
[26] J. Scheuring, J. Lee, M. Cushman, H. Patel, D.A. Patrick, A. Bacher, (Trifluoromethyl)Lumazine derivatives as ^{19}F NMR probes for Lumazine Protein, Biochemistry 33 (1994) 7634–7640.
[27] J.F. Eccleston, D.P. Molloy, M.G. Hinds, R.W. King, J. Feeney, Conformational differences between complexes of elongation-factor Tu studied by ^{19}F-NMR spectroscopy, Eur. J. Biochem. 218 (1993) 1041–1047.
[28] L. McDowell, M. Lee, R.A. McKay, K.S. Anderson, J. Schaefer, Intersubunit communication in tryptophan synthase by carbon-13 and fluorine-19 REDOR NMR, Biochemistry 35 (1996) 3328–3334.
[29] L.M. McDowell, S.M. Holl, S. Qian, E. Li, J. Schaefer, Inter-tryptophan distances in rat cellular retinol binding protein II by solid-state NMR, Biochemistry 32 (1993) 4560–4563.
[30] M.A. Danielson, J.J. Falke, Use of ^{19}F NMR to probe protein structure and conformational changes, Annu. Rev. Biophys. Biomol. Struct. 25 (1996) 163–195.
[31] L.A. Luck, J.E. Vance, T.M. O'Connell, R.E. London, ^{19}F NMR relaxation studies on 5-fluorotryptophan- and tetradeutero-5-fluorotryptophan-labeled *E. coli* glucose/galactose receptor, J. Biomol. NMR 7 (1996) 261–272.
[32] C.A. Klug, K. Tasaki, N. Tjandra, C. Ho, J. Schaefer, Closed form of liganded glutamine-binding protein by rotational-echo double-resonance NMR, Biochemistry 36 (1997) 9405–9408.
[33] E.Y. Lau, J.T. Gerig, Effects of fluorine substitution on the structure and dynamics of complexes of dihydrofolate reductase (*Escherichia coli*), Biophys. J. 73 (1997) 1579–1592.
[34] M. Bouchard, C. Paré, J.P. Dutasta, J.P. Chauvet, C. Gicquaud, M. Auger, Interaction between G-actin and various types of liposomes: A ^{19}F, ^{31}P, and ^{2}H nuclear magnetic resonance study, Biochemistry 37 (1998) 3149–3155.
[35] J.M. Goetz, B. Poliks, D.R. Studelska, M. Fischer, K. Kegelbrey, A. Bacher, M. Cushman, J. Schaefer, Investigation of the binding of fluorolumazines to the 1-MDa capsid of lumazine synthase by ^{15}N{^{19}F} REDOR NMR, J. Am. Chem. Soc. 121 (1999) 7500–7508.
[36] G. Anderluh, A. Razpotnik, Z. Podlesek, P. Macek, F. Separovic, R.S. Norton, Interaction of the eukaryotic pore-forming cytolysin

equinatoxin II with model membranes: ^{19}F NMR studies, J. Mol. Biol. 347 (2005) 27–39.

[37] J. Feeney, J.E. McCormick, C.J. Bauer, B. Birdsall, C.M. Moody, B.A. Starkmann, D.W. Young, P. Francis, R.H. Havlin, W.D. Arnold, E. Oldfield, ^{19}F nuclear magnetic resonance chemical shifts of fluorine containing aliphatic amino acids in proteins: studies on *Lactobacillus casei* dihydrofolate reductase containing (2*S*,4*S*)-5-fluoroleucine, J. Am. Chem. Soc. 118 (1996) 8700–8706.

[38] E.Y. Lau, J.T. Gerig, Effects of fluorine substitution on the structure and dynamics of complexes of dihydrofolate reductase (*Escherichia coli*), Biophys. J. 73 (1997) 1579–1592.

[39] S.L. Grage, J.F. Wang, T.A. Cross, A.S. Ulrich, Solid-state ^{19}F NMR analysis of ^{19}F-labeled tryptophan in gramicidin A in oriented membranes, Biophys. J. 83 (2002) 3336–3350.

[40] J. Salgado, S.L. Grage, L.H. Kondejewski, R.S. Hodges, R.N. McElhaney, A.S. Ulrich, Membrane-bound structure and alignment of the antimicrobial β-sheet peptide gramicidin S derived from angular and distance constraints by solid state ^{19}F NMR, J. Biomol. NMR 21 (2001) 191–208.

[41] S. Afonin, R.W. Glaser, M. Berditchevskaia, P. Wadhwani, K.H. Gührs, U. Möllmann, A. Perner, A.S. Ulrich, 4-Fluorophenylglycine as a label for ^{19}F NMR structure analysis of membrane-associated peptides, ChemBioChem 4 (2003) 1151–1163.

[42] S. Afonin, P.K. Mikhailiuk, I.V. Komarov, A.S. Ulrich, Evaluating the use of CF_3-bicyclopentylglycine as a label for ^{19}F NMR structure analysis of membrane-bound peptides, J. Pept. Sci. 13 (2007) 614–623.

[43] S.L. Grage, U. Dürr, S. Afonin, P.K. Mikhailiuk, I.V. Komarov, A.S. Ulrich, Solid-state ^{19}F NMR parameters of fluorine-labeled amino acids (Part II): aliphatic substituents, J. Magn. Reson. 191 (2008) 16–23.

[44] J. Herzfeld, A.E. Berger, Sideband intensities in NMR-spectra of samples spinning at the magic angle, J. Chem. Phys. 73 (1980) 6021–6030.

[45] P. Hodgkinson, L. Emsley, The reliability of the determination of tensor parameters by solid-state nuclear magnetic resonance, J. Chem. Phys. 107 (1997) 4808–4816.

[46] W.S. Brey, M.L. Brey, Fluorine-19 NMR, in: D.M. Grant, R.K. Harris (Eds.), Encyclopedia of NMR, Wiley, New York, 1996, pp. 2063–2071.

[47] S. Berger, S. Braun, H.-O. Kalinowski, NMR-Spektroskopie von Nichtmetallen; Band 4: ^{19}F NMR Spektroskopie, Georg Thieme Verlag, Stuttgart, 1992.

[48] S.P. Graether, J.S. DeVries, R. McDonald, M.L. Rakovszky, B.D. Sykes, A ^{1}H/^{19}F minicoil NMR probe for solid-state NMR: application to 5-fluoroindoles, J. Magn. Reson. 178 (2006) 65–71.

[49] X. Zhao, J.S. DeVries, R. McDonald, B.D. Sykes, Determination of the ^{19}F NMR chemical shielding tensor and crystal structure of 5-fluoro-DL-tryptophan, J. Magn. Reson. 187 (2007) 88–96.

[50] M.H. Frey, J.A. Diverdi, S.J. Opella, Dynamics of phenylalanine in the solid-state by NMR, J. Am. Chem. Soc. 107 (1985) 7311–7315.

[51] W. Luo, M. Hong, Determination of the oligomeric number and intermolecular distances of membrane protein assemblies by anisotropic H-1-driven spin diffusion NMR spectroscopy, J. Am. Chem. Soc. 128 (2006) 7242–7251.

[52] M. Cotten, C. Tian, D.D. Busath, R.B. Shirts, T.A. Cross, Modulating dipoles for structure-function correlations in the gramicidin A channel, Biochemistry 38 (1999) 9185–9197.

[53] R. Campos-Olivas, R. Aziz, G.L. Helms, J.N.S. Evans, A.M. Gronenborn, Placement of ^{19}F into the center of GB1: effects on structure and stability, FEBS Lett. 517 (2002) 55–60.

[54] S. D. Müller, In vivo Markierung der Proteine GB1 und TatA mit Fluorderivaten aromatischer Aminosäuren, Diploma Thesis, University of Karlsruhe, 2004.